

ORIGINAL ARTICLE

Pulmonary Vascular Endothelialitis, Thrombosis, and Angiogenesis in Covid-19

Maximilian Ackermann, M.D., Stijn E. Verleden, Ph.D., Mark Kuehnel, Ph.D., Axel Haverich, M.D., Tobias Welte, M.D., Florian Laenger, M.D., Arno Vanstapel, Ph.D., Christopher Werlein, M.D., Helge Stark, Ph.D., Alexandar Tzankov, M.D., William W. Li, M.D., Vincent W. Li, M.D., Steven J. Mentzer, M.D., and Danny Jonigk, M.D.

ABSTRACT

BACKGROUND

Progressive respiratory failure is the primary cause of death in the coronavirus disease 2019 (Covid-19) pandemic. Despite widespread interest in the pathophysiology of the disease, relatively little is known about the associated morphologic and molecular changes in the peripheral lung of patients who die from Covid-19.

METHODS

We examined 7 lungs obtained during autopsy from patients who died from Covid-19 and compared them with 7 lungs obtained during autopsy from patients who died from acute respiratory distress syndrome (ARDS) secondary to influenza A(H1N1) infection and 10 age-matched, uninfected control lungs. The lungs were studied with the use of seven-color immunohistochemical analysis, micro-computed tomographic imaging, scanning electron microscopy, corrosion casting, and direct multiplexed measurement of gene expression.

RESULTS

In patients who died from Covid-19–associated or influenza-associated respiratory failure, the histologic pattern in the peripheral lung was diffuse alveolar damage with perivascular T-cell infiltration. The lungs from patients with Covid-19 also showed distinctive vascular features, consisting of severe endothelial injury associated with the presence of intracellular virus and disrupted cell membranes. Histologic analysis of pulmonary vessels in patients with Covid-19 showed widespread thrombosis with microangiopathy. Alveolar capillary microthrombi were 9 times as prevalent in patients with Covid-19 as in patients with influenza ($P<0.001$). In lungs from patients with Covid-19, the amount of new vessel growth — predominantly through a mechanism of intussusceptive angiogenesis — was 2.7 times as high as that in the lungs from patients with influenza ($P<0.001$).

CONCLUSIONS

In our small series, vascular angiogenesis distinguished the pulmonary pathobiology of Covid-19 from that of equally severe influenza virus infection. The universality and clinical implications of our observations require further research to define. (Funded by the National Institutes of Health and others.)

From the Institute of Pathology and Department of Molecular Pathology, Helios University Clinic Wuppertal, University of Witten–Herdecke, Wuppertal (M.A.), the Institute of Functional and Clinical Anatomy, University Medical Center of the Johannes Gutenberg University Mainz, Mainz (M.A.), the Institute of Pathology (M.K., F.L., C.W., H.S., D.J.), the Department of Cardiothoracic, Transplantation, and Vascular Surgery (A.H.), and the Clinic of Pneumology (T.W.), Hannover Medical School, and the German Center for Lung Research, Biomedical Research in Endstage and Obstructive Lung Disease Hannover (BREATH) (M.K., A.H., T.W., F.L., C.W., H.S., D.J.), Hannover — all in Germany; the Laboratory of Respiratory Diseases, BREATH, Department of Chronic Diseases, Metabolism, and Aging, KU Leuven, Leuven, Belgium (S.E.V., A.V.); the Institute of Pathology and Medical Genetics, University Hospital Basel, Basel, Switzerland (A.T.); and the Angiogenesis Foundation, Cambridge (W.W.L., V.W.L.), and the Laboratory of Adaptive and Regenerative Biology and the Division of Thoracic Surgery, Brigham and Women's Hospital, Harvard Medical School, Boston (S.J.M.) — all in Massachusetts. Address reprint requests to Dr. Mentzer at the Division of Thoracic Surgery, Brigham and Women's Hospital, Harvard Medical School, 75 Francis St., Boston, MA 02115, or at smentzer@bwh.harvard.edu.

This article was published on May 21, 2020, at NEJM.org.

DOI: 10.1056/NEJMoa2015432

Copyright © 2020 Massachusetts Medical Society.

INFECTION WITH SEVERE ACUTE RESPIRATORY syndrome coronavirus 2 (SARS-CoV-2) in humans is associated with a broad spectrum of clinical respiratory syndromes, ranging from mild upper airway symptoms to progressive life-threatening viral pneumonia.^{1,2} Clinically, patients with severe coronavirus disease 2019 (Covid-19) have labored breathing and progressive hypoxemia and often receive mechanical ventilatory support. Radiographically, peripheral lung ground-glass opacities on computed tomographic (CT) imaging of the chest fulfill the Berlin criteria for acute

respiratory distress syndrome (ARDS).^{3,4} Histologically, the hallmark of the early phase of ARDS is diffuse alveolar damage with edema, hemorrhage, and intraalveolar fibrin deposition, as described by Katzenstein et al.⁵ Diffuse alveolar damage is a nonspecific finding, since it may have noninfectious or infectious causes, including Middle East respiratory syndrome coronavirus (MERS-CoV),⁶ SARS-CoV,⁷ SARS-CoV-2,⁸⁻¹⁰ and influenza viruses.¹¹

Among the distinctive features of Covid-19 are the vascular changes associated with the disease. With respect to diffuse alveolar damage in SARS-CoV⁷ and SARS-CoV-2 infection,^{8,12} the formation of fibrin thrombi has been observed anecdotally but not studied systematically. Clinically, many patients have elevated D-dimer levels, as well as cutaneous changes in their extremities suggesting thrombotic microangiopathy.¹³ Diffuse intravascular coagulation and large-vessel thrombosis have been linked to multisystem organ failure.¹⁴⁻¹⁶ Peripheral pulmonary vascular changes are less well characterized; however, vasculopathy in the gas-exchange networks, depending on its effect on the matching of ventilation and perfusion that results, could potentially contribute to hypoxemia and the effects of posture (e.g., prone positioning) on oxygenation.¹⁷

Despite previous experience with SARS-CoV¹⁸ and early experience with SARS-CoV-2, the mor-

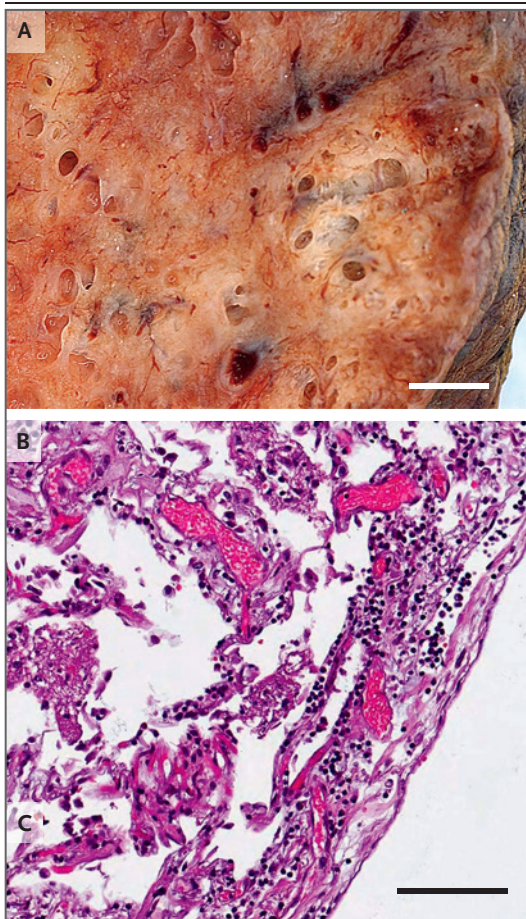


Figure 1. Lymphocytic Inflammation in a Lung from a Patient Who Died from Covid-19.

The gross appearance of a lung from a patient who died from coronavirus disease 2019 (Covid-19) is shown in Panel A (the scale bar corresponds to 1 cm). The histopathological examination, shown in Panel B, revealed interstitial and perivascular predominantly lymphocytic pneumonia with multifocal endothelialitis (hematoxylin–eosin staining; the scale bar corresponds to 200 μ m).

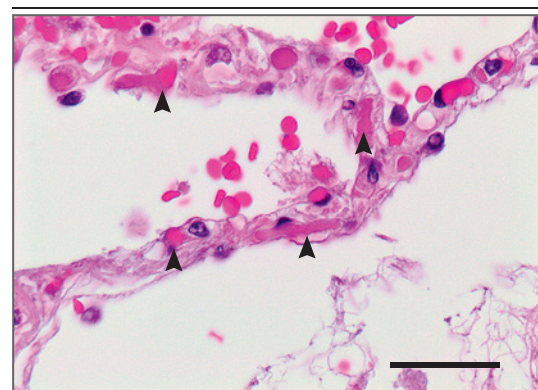


Figure 2. Microthrombi in the Interalveolar Septa of a Lung from a Patient Who Died from Covid-19.

The interalveolar septum of this patient (Patient 4 in Table S1A in the Supplementary Appendix) shows slightly expanded alveolar walls with multiple fibrinous microthrombi (arrowheads) in the alveolar capillaries. Extravasated erythrocytes and a loose network of fibrin can be seen in the intraalveolar space (hematoxylin–eosin staining; the scale bar corresponds to 50 μ m).

phologic and molecular changes associated with these infections in the peripheral lung are not well documented. Here, we examine the morphologic and molecular features of lungs obtained during autopsy from patients who died from Covid-19, as compared with those of lungs from patients who died from influenza and age-matched, uninfected control lungs.

METHODS

PATIENT SELECTION AND WORKFLOW

We analyzed pulmonary autopsy specimens from seven patients who died from respiratory failure caused by SARS-CoV-2 infection and compared them with lungs from seven patients who died from pneumonia caused by influenza A virus

subtype H1N1 (A[H1N1]) — a strain associated with the 1918 and 2009 influenza pandemics. The lungs from patients with influenza were archived tissue from the 2009 pandemic and were chosen for the best possible match with respect to age, sex, and disease severity from among the autopsies performed at the Hannover Medical School. Ten lungs that had been donated but not used for transplantation served as uninfected control specimens. The Covid-19 group consisted of lungs from two female and five male patients with mean (\pm SD) ages of 68 ± 9.2 years and 80 ± 11.5 years, respectively (clinical data are provided in Table S1A in the Supplementary Appendix, available with the full text of this article at NEJM.org). The influenza group consisted of lungs from two female and five male patients

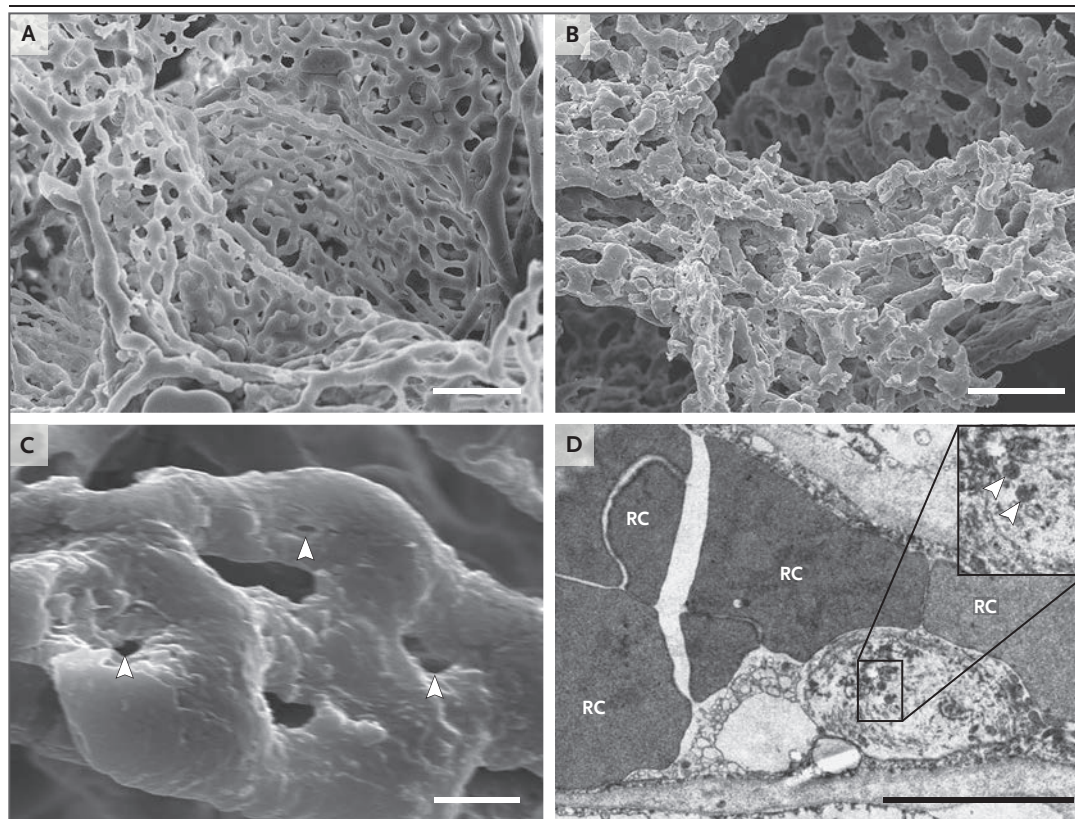
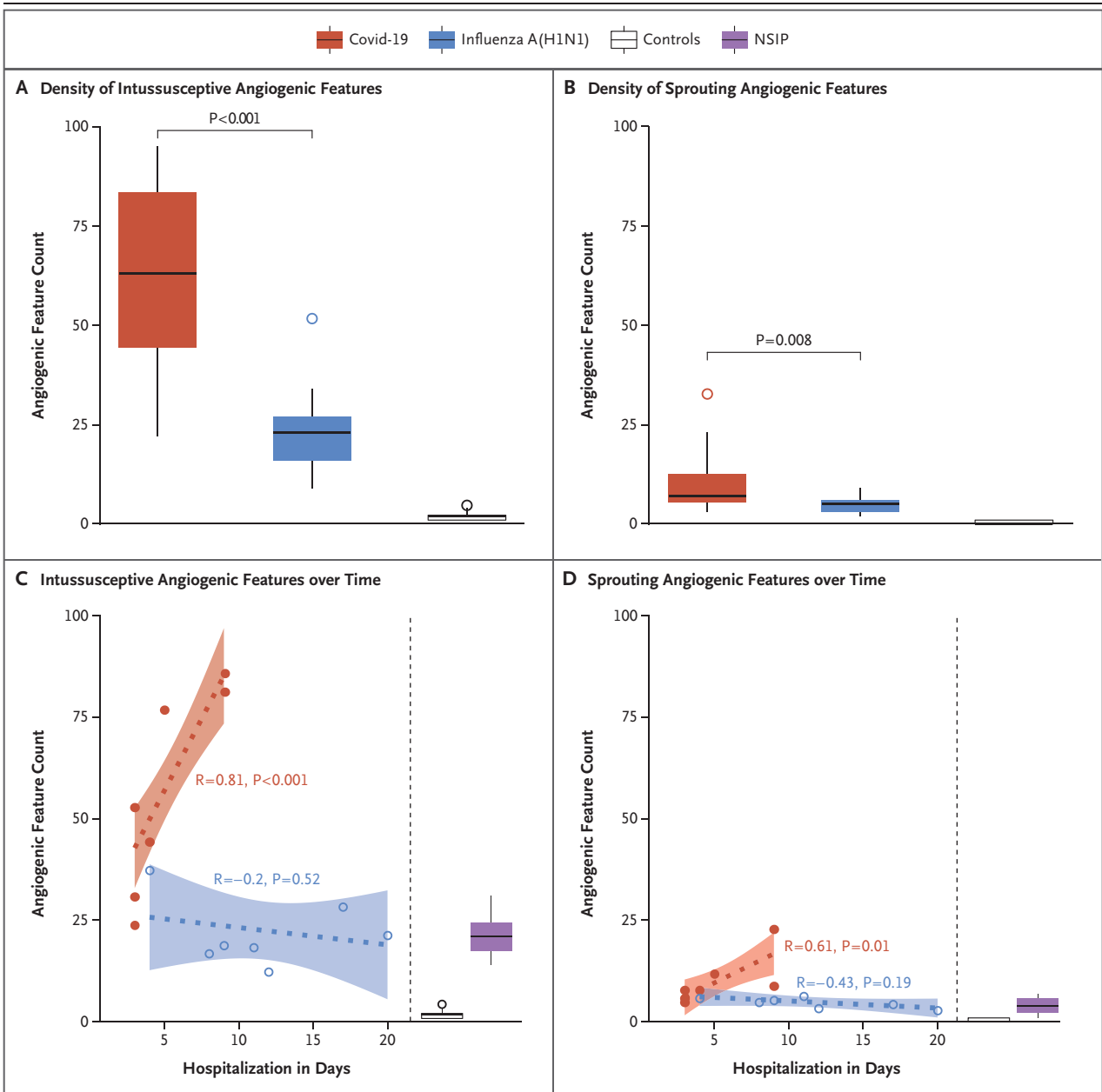


Figure 3. Microvascular Alterations in Lungs from Patients Who Died from Covid-19.

Panels A and B show scanning electron micrographs of microvascular corrosion casts from the thin-walled alveolar plexus of a healthy lung (Panel A) and the substantial architectural distortion seen in lungs injured by Covid-19 (Panel B). The loss of a clearly visible vessel hierarchy in the alveolar plexus is the result of new blood-vessel formation by intussusceptive angiogenesis. Panel C shows the intussusceptive pillar localizations (arrowheads) at higher magnification. Panel D is a transmission electron micrograph showing ultrastructural features of endothelial cell destruction and SARS-CoV-2 visible within the cell membrane (arrowheads) (the scale bar corresponds to 5 μ m). RC denotes red cell.



with mean ages of 62.5 ± 4.9 years and 55.4 ± 10.9 years, respectively. Five of the uninfected lungs were from female donors (mean age, 68.2 ± 6.9 years), and five were from male donors (mean age, 79.2 ± 3.3 years) (clinical data are provided in Table S1B). The study was approved by and conducted according to requirements of the ethics committees at the Hannover Medical School and the University of Leuven. There was no commercial support for this study.

All lungs were comprehensively analyzed with the use of microCT, histopathological, and multi-

plexed immunohistochemical analysis, transmission and scanning electron microscopy, corrosion casting, and direct multiplexed gene-expression analysis, as described in detail in the Methods section in the Supplementary Appendix.

STATISTICAL ANALYSIS

All comparisons of numeric variables (including those in the gene-expression analysis) were conducted with Student's t-test familywise error rates due to multiplicity set at 0.05 with the use of the Benjamini-Hochberg method of controlling false

Figure 4 (facing page). Numeric Density of Features of Intussusceptive and Sprouting Angiogenesis in Lungs from Patients Who Died from Covid-19 or Influenza A(H1N1).

Angiogenic features of sprouting and intussusceptive angiogenesis (intussusceptive pillars and sprouts, respectively) were counted per field of view in microvascular corrosion casts of lungs from patients with Covid-19 (red), lungs from patients with influenza A(H1N1) (blue), and control lungs (white). In Panels A and B, the numeric densities of angiogenic features are summarized as box plots for intussusceptive and sprouting angiogenesis. The boxes reflect the interquartile range, and the whiskers indicate the range (up to 1.5 times the interquartile range). Outliers are denoted by singular points. A statistical comparison between lungs from patients Covid-19 and those from patients with influenza and uninfected control lungs showed a significantly higher frequency of angiogenesis in the patients with Covid-19 lungs, especially intussusceptive angiogenesis (P values were calculated with Student's t-test, controlled for the familywise error rate with a Benjamini-Hochberg false discovery rate threshold of 0.05). Panels C and D show a chronological comparison of intussusceptive and sprouting angiogenesis in lungs from patients with Covid-19 and lungs from patients with influenza A(H1N1) plotted as a function of the duration of hospitalization. The numbers shown are Pearson correlation coefficients and P values (all displayed P values of 0.05 or lower also pass the false discovery rate threshold of 0.05). The median angiogenic feature count for each patient is displayed as one dot. The shaded areas encompassing the dotted linear regression lines are smoothed 95% confidence intervals. As a reference for increased blood-vessel formation in lung diseases, intussusceptive and sprouting angiogenesis as found in end-stage nonspecific interstitial pneumonia (NSIP), a chronic interstitial lung disease, at the time of lung transplantation (a mean of 1650 days from first consultation to lung transplantation) are shown (purple box plots). Findings in healthy control lungs are also indicated (white box plots). The white and purple box plots are displayed in relation to the y axis but not the x axis (as indicated by vertical dashed lines).

discovery rates. Original P values are reported only for the tests that met the criteria for false discovery rates. All confidence intervals have been calculated on the basis of the t-distribution, as well. Additional details are provided in the Methods section of the Supplementary Appendix.

RESULTS

GROSS EXAMINATION

The mean (\pm SE) weight of the lungs from patients with proven influenza pneumonia was significantly higher than that from patients with proven

Covid-19 (2404 ± 560 g vs. 1681 ± 49 g; $P=0.04$). The mean weight of the uninfected control lungs (1045 ± 91 g) was significantly lower than those in the influenza group ($P=0.003$) and the Covid-19 group ($P<0.001$).

ANGIOCENTRIC INFLAMMATION

All lung specimens from the Covid-19 group had diffuse alveolar damage with necrosis of alveolar lining cells, pneumocyte type 2 hyperplasia, and linear intraalveolar fibrin deposition (Fig. 1). In four of seven cases, the changes were focal, with only mild interstitial edema. The remaining three cases had homogeneous fibrin deposits and marked interstitial edema with early intraalveolar organization. The specimens in the influenza group had florid diffuse alveolar damage with massive interstitial edema and extensive fibrin deposition in all cases. In addition, three specimens in the influenza group had focal organizing and resorptive inflammation (Fig. S2). These changes were reflected in the much higher weight of the lungs from patients with influenza.

Immunohistochemical analysis of angiotensin-converting enzyme 2 (ACE2) expression, measured as mean (\pm SD) relative counts of ACE2-positive cells per field of view, in uninfected control lungs showed scarce expression of ACE2 in alveolar epithelial cells (0.053 ± 0.03) and capillary endothelial cells (0.066 ± 0.03). In lungs from patients with Covid-19 and lungs from patients with influenza, the relative counts of ACE2-positive cells per field of view were 0.25 ± 0.14 and 0.35 ± 0.15 , respectively, for alveolar epithelial cells and 0.49 ± 0.28 and 0.55 ± 0.11 , respectively, for endothelial cells. Furthermore, ACE2-positive lymphocytes were not seen in perivascular tissue or in the alveoli of the control lungs but were present in the lungs in the Covid-19 group and the influenza group (relative counts of 0.22 ± 0.18 and 0.15 ± 0.09 , respectively). (Details of counting are provided in Table S2.)

In the lungs from patients with Covid-19 and patients with influenza, similar mean (\pm SD) numbers of CD3-positive T cells were found within a $200\text{-}\mu\text{m}$ radius of precapillary and postcapillary vessel walls in 20 fields of examination per patient (26.2 ± 13.1 for Covid-19 and 14.8 ± 10.8 for influenza). With the same field size used for examination, CD4-positive T cells were more numerous in lungs from patients with Covid-19 than in lungs from patients with influenza (13.6 ± 6.0

vs. 5.8 ± 2.5 , $P=0.04$), whereas CD8-positive T cells were less numerous (5.3 ± 4.3 vs. 11.6 ± 4.9 , $P=0.008$). Neutrophils (CD15 positive) were significantly less numerous adjacent to the alveolar epithelial lining in the Covid-19 group than in the influenza group (0.4 ± 0.5 vs. 4.8 ± 5.2 , $P=0.002$).

A multiplexed analysis of inflammation-related gene expression examining 249 genes from the nCounter Inflammation Panel (NanoString Technologies) revealed similarities and differences between the specimens in the Covid-19 group and those in the influenza group. A total of 79

inflammation-related genes were differentially regulated only in specimens from patients with Covid-19, whereas 2 genes were differentially regulated only in specimens from patients with influenza; a shared expression pattern was found for 7 genes (Fig. S1).

THROMBOSIS AND MICROANGIOPATHY

The pulmonary vasculature of the lungs in the Covid-19 group and the influenza group was analyzed with hematoxylin–eosin, trichrome, and immunohistochemical staining (as described in

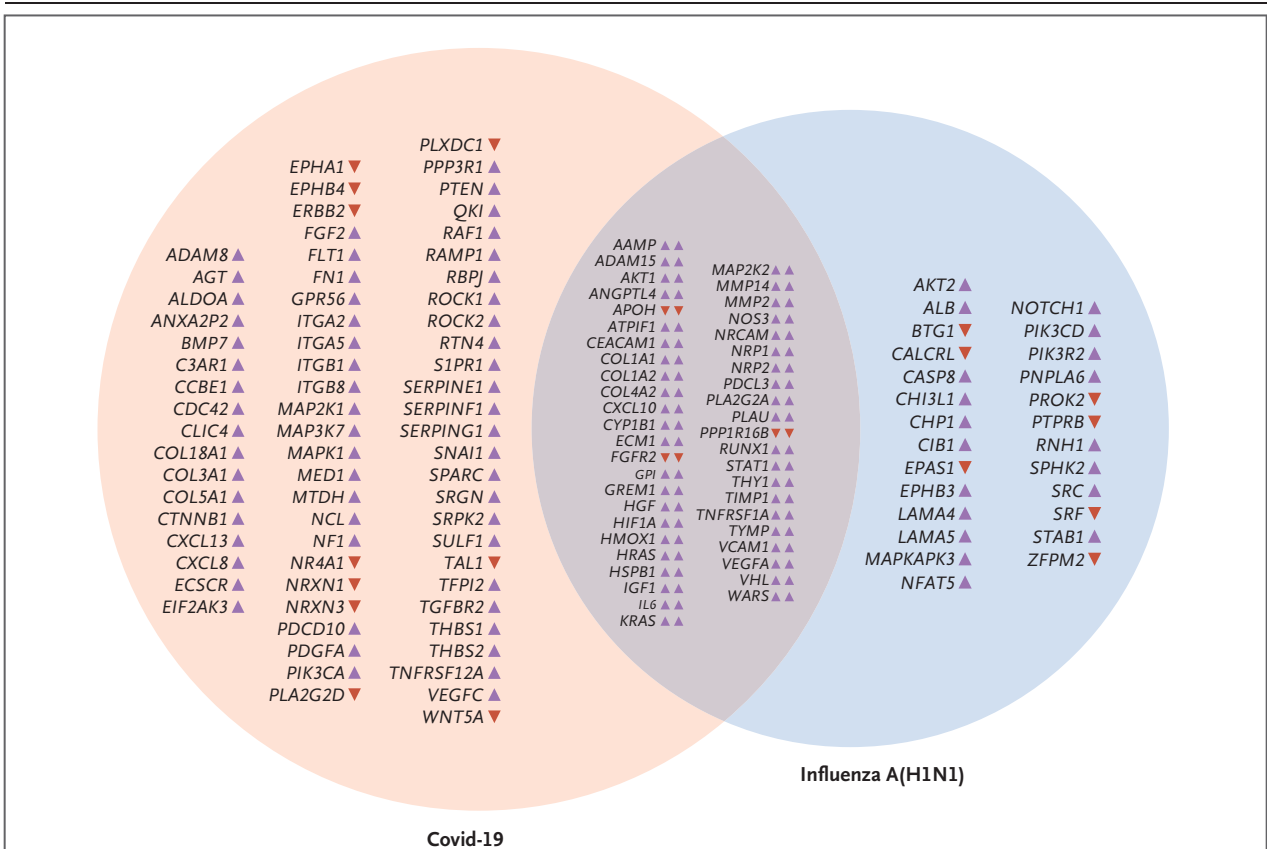


Figure 5. Relative Expression Analysis of Angiogenesis-Associated Genes in Lungs from Patients Who Died from Covid-19 or Influenza A(H1N1).

RNA was isolated from sections sampled directly adjacent to those used for complementary histologic and immunohistochemical analyses. RNA was isolated with the Maxwell RNA extraction system (Promega) and, after quality control through Qubit analysis (ThermoFisher), was used for further analysis. During the NanoString procedure, individual copies of all RNA molecules were labeled with gene-specific bar codes and counted individually with the nCounter Analysis System (NanoString Technologies). The expression of angiogenesis-associated genes was measured with the NanoString nCounter PanCancer Progression panel (323 target genes annotated as relevant for angiogenesis). The resulting gene-expression data were normalized to negative control lanes (arithmetic mean background subtraction), positive control lanes (geometric mean normalization factor), and all reference genes present on the panel (geometric mean normalization factor) with the use of nSolver Analysis Software, version 4.0. Shown in the Venn diagram are only genes that are statistically differentially expressed as compared with expression in controls in both disease groups (Student’s t-test, controlled for the familywise error rate with a Benjamini–Hochberg false discovery rate threshold of 0.05). Up-regulation and down-regulation of genes is indicated by colored arrowheads suffixed to the gene symbols (purple denotes up-regulation, red denotes down-regulation).

the Methods section of the Supplementary Appendix). Analysis of precapillary vessels showed that in four of the seven lungs from patients with Covid-19 and four of the seven lungs from the patients with influenza, thrombi were consistently present in pulmonary arteries with a diameter of 1 mm to 2 mm, without complete luminal obstruction (Figs. S3 and S5). Fibrin thrombi of the alveolar capillaries could be seen in all the lungs from both groups of patients (Fig. 2). Alveolar capillary microthrombi were 9 times as prevalent in patients with Covid-19 as in patients with influenza (mean [\pm SD] number of distinct thrombi per square centimeter of vascular lumen area, 159 ± 73 and 16 ± 16 , respectively; $P=0.002$). Intravascular thrombi in postcapillary venules of less than 1 mm diameter were seen in lower numbers in the lungs from patients with Covid-19 than in those from patients with influenza (12 ± 14 vs. 35 ± 16 , $P=0.02$). Two lungs in the Covid-19 group had involvement of all segments of the vasculature, as compared with four of the lungs in the influenza group; in three of the lungs in the Covid-19 group and three of the lungs in the influenza group, combined capillary and venous thrombi were found without arterial thrombi.

The histologic findings were supported by three-dimensional microCT of the pulmonary specimens: the lungs from patients with Covid-19 and from patients with influenza showed nearly total occlusions of precapillary and postcapillary vessels.

ANGIOGENESIS

We examined the microvascular architecture of the lungs from patients with Covid-19, lungs from patients with influenza, and uninfected control lungs with the use of scanning electron microscopy and microvascular corrosion casting. The lungs in the Covid-19 group had a distorted vascularity with structurally deformed capillaries (Fig. 3). Elongated capillaries in the lungs from patients with Covid-19 showed sudden changes in caliber and the presence of intussusceptive pillars within the capillaries (Fig. 3C). Transmission electron microscopy of the Covid-19 endothelium showed ultrastructural damage to the endothelium, as well as the presence of intracellular SARS-CoV-2 (Fig. 3D). The virus could also be identified in the extracellular space.

In the lungs from patients with Covid-19, the density of intussusceptive angiogenic features

(mean [\pm SE], 60.7 ± 11.8 features per field) was significantly higher than that in lungs from patients with influenza (22.5 ± 6.9) or in uninfected control lungs (2.1 ± 0.6) ($P<0.001$ for both comparisons) (Fig. 4A). The density of features of conventional sprouting angiogenesis was also higher in the Covid-19 group than in the influenza group (Fig. 4B). When the pulmonary angiogenic feature count was plotted as a function of the length of hospital stay, the degree of intussusceptive angiogenesis was found to increase significantly with increasing duration of hospitalization ($P<0.001$) (Fig. 4C). In contrast, the lungs from patients with influenza had less intussusceptive angiogenesis and no increase over time (Fig. 4C). A similar pattern was seen for sprouting angiogenesis (Fig. 4D).

A multiplexed analysis of angiogenesis-related gene expression examining 323 genes from the nCounter PanCancer Progression Panel (NanoString Technologies) revealed differences between the specimens from patients with Covid-19 and those from patients with influenza. A total of 69 angiogenesis-related genes were differentially regulated only in the Covid-19 group, as compared with 26 genes differentially regulated only in the influenza group; 45 genes had shared changes in expression (Fig. 5).

DISCUSSION

In this study, we examined the morphologic and molecular features of seven lungs obtained during autopsy from patients who died from SARS-CoV-2 infection. The lungs from these patients were compared with those obtained during autopsy from patients who had died from ARDS secondary to influenza A(H1N1) infection and from uninfected controls. The lungs from the patients with Covid-19 and the patients with influenza shared a common morphologic pattern of diffuse alveolar damage and infiltrating perivascular lymphocytes. There were three distinctive angiocentric features of Covid-19. The first feature was severe endothelial injury associated with intracellular SARS-CoV-2 virus and disrupted endothelial cell membranes. Second, the lungs from patients with Covid-19 had widespread vascular thrombosis with microangiopathy and occlusion of alveolar capillaries.^{12,19} Third, the lungs from patients with Covid-19 had significant new vessel growth through a mechanism of intussus-

ceptive angiogenesis. Although our sample was small, the vascular features we identified are consistent with the presence of distinctive pulmonary vascular pathobiologic features in some cases of Covid-19.

Our finding of enhanced intussusceptive angiogenesis in the lungs from patients with Covid-19 as compared with the lungs from patients with influenza was unexpected. New vessel growth can occur by conventional sprouting or intussusceptive (nonsprouting) angiogenesis. The characteristic feature of intussusceptive angiogenesis is the presence of a pillar or post spanning the lumen of the vessel.²⁰ Typically referred to as an intussusceptive pillar, this endothelial-lined intravascular structure is not seen by light microscopy but is readily identifiable by corrosion casting and scanning electron microscopy.²¹ Although tissue hypoxia was probably a common feature in the lungs from both these groups of patients, we speculate that the greater degree of endothelialitis and thrombosis in the lungs from patients with Covid-19 may contribute to the relative frequency of sprouting and intussusceptive angiogenesis observed in these patients. The relationship of these findings to the clinical course of Covid-19 requires further research to elucidate.

A major limitation of our study is that the sample was small; we studied only 7 patients among the more than 320,000 people who have died from Covid-19, and the autopsy data also represent static information. On the basis of the available data, we cannot reconstruct the timing of death in the context of an evolving disease process. Moreover, there could be other factors that account for the differences we observed between patients with Covid-19 and those with influenza. For example, none of the patients in our study who died from Covid-19 had been treated with standard mechanical ventilation, whereas five of the seven patients who died from influenza had received pressure-controlled ventilation. Similarly, it is possible that differences in detectable intussusceptive angiogenesis could be due to the different time courses of Covid-19 and influenza. These and other unknown factors must be considered when evaluating our data.²² Nonetheless, our analysis suggests that this possibility is unlikely, particularly since the degree of

intussusceptive angiogenesis in the patients with Covid-19 increased significantly with increasing length of hospitalization, whereas in the patients with influenza it remained stable at a significantly lower level. Moreover, we have shown intussusceptive angiogenesis to be the predominant angiogenic mechanism even in late stages of chronic lung injury.²¹

ACE2 is an integral membrane protein that appears to be the host-cell receptor for SARS-CoV-2.^{23,24} Our data showed significantly greater numbers of ACE2-positive cells in the lungs from patients with Covid-19 and from patients with influenza than in those from uninfected controls. We found greater numbers of ACE2-positive endothelial cells and significant changes in endothelial morphology, a finding consistent with a central role of endothelial cells in the vascular phase of Covid-19. Endothelial cells in the specimens from patients with Covid-19 showed disruption of intercellular junctions, cell swelling, and a loss of contact with the basal membrane. The presence of SARS-CoV-2 virus within the endothelial cells, a finding consistent with other studies,²⁵ suggests that direct viral effects as well as perivascular inflammation may contribute to the endothelial injury.

We report the presence of pulmonary intussusceptive angiogenesis and other pulmonary vascular features in the lungs of seven patients who died from Covid-19. Additional work is needed to relate our findings to the clinical course in these patients. To aid others in their research, our full data set is available on the Vivli platform (<https://vivli.org/>) and can be requested with the use of the following digital object identifier: <https://doi.org/10.25934/00005576>.

Supported by grants (HL94567 and HL134229, to Drs. Ackermann and Mentzer) from the National Institutes of Health, a grant from the Botnar Research Centre for Child Health (to Dr. Tzankov), a European Research Council Consolidator Grant (XHale) (771883, to Dr. Jonigk), and a grant (KFO311, to Dr. Jonigk) from Deutsche Forschungsgemeinschaft (Project Z2).

Disclosure forms provided by the authors are available with the full text of this article at NEJM.org.

We thank Kerstin Bahr, Jan Hinrich Braesen, Peter Braubach, Emily Brouwer, Annette Mueller Brechlin, Regina Engelhardt, Jasmin Haslbauer, Anne Hofer, Nicole Kroenke, Thomas Menter, Mahtab Taleb Naghsh, Christina Petzold, Vincent Schmidt, and Pauline Tittmann for technical support; Peter Boor of the German Covid-19 registry; and Lynnette Sholl, Hans Kreipe, Hans Michael Kvasnicka, and Jean Connors for helpful comments. Dr. Jonigk thanks Anita Swiatlak for her continued support.

REFERENCES

1. Zhu N, Zhang D, Wang W, et al. A novel coronavirus from patients with pneumonia in China, 2019. *N Engl J Med* 2020;382:727-33.
2. Chen N, Zhou M, Dong X, et al. Epidemiological and clinical characteristics of 99 cases of 2019 novel coronavirus pneumonia in Wuhan, China: a descriptive study. *Lancet* 2020;395:507-13.
3. Raptis CA, Hammer MM, Short RG, et al. Chest CT and coronavirus disease (COVID-19): a critical review of the literature to date. *AJR Am J Roentgenol* 2020 April 16 (Epub ahead of print).
4. Thompson BT, Chambers RC, Liu KD. Acute respiratory distress syndrome. *N Engl J Med* 2017;377:562-72.
5. Katzenstein AL, Bloor CM, Leibov AA. Diffuse alveolar damage — the role of oxygen, shock, and related factors: a review. *Am J Pathol* 1976;85:209-28.
6. Alsaad KO, Hajeer AH, Al Balwi M, et al. Histopathology of Middle East respiratory syndrome coronavirus (MERS-CoV) infection — clinicopathological and ultrastructural study. *Histopathology* 2018; 72:516-24.
7. Nicholls JM, Poon LLM, Lee KC, et al. Lung pathology of fatal severe acute respiratory syndrome. *Lancet* 2003;361:1773-8.
8. Barton LM, Duval EJ, Stroberg E, Ghosh S, Mukhopadhyay S. COVID-19 autopsies, Oklahoma, USA. *Am J Clin Pathol* 2020;153:725-33.
9. Tian S, Hu W, Niu L, Liu H, Xu H, Xiao SY. Pulmonary pathology of early-phase 2019 novel coronavirus (COVID-19) pneumonia in two patients with lung cancer. *J Thorac Oncol* 2020;15:700-4.
10. Menter T, Haslbauer JD, Nienhold R, et al. Post-mortem examination of COVID-19 patients reveals diffuse alveolar damage with severe capillary congestion and variegated findings of lungs and other organs suggesting vascular dysfunction. *Histopathology* 2020 May 4 (Epub ahead of print).
11. Voltersvik P, Aqrabi LA, Dudman S, et al. Pulmonary changes in Norwegian fatal cases of pandemic influenza H1N1 (2009) infection: a morphologic and molecular genetic study. *Influenza Other Respir Viruses* 2016;10:525-31.
12. Magro C, Mulvey JJ, Berlin D, et al. Complement associated microvascular injury and thrombosis in the pathogenesis of severe COVID-19 infection: a report of five cases. *Transl Res* 2020 April 15 (Epub ahead of print).
13. Liu PP, Blet A, Smyth D, Li H. The science underlying COVID-19: implications for the cardiovascular system. *Circulation* 2020 April 15 (Epub ahead of print).
14. Tang N, Bai H, Chen X, Gong J, Li D, Sun Z. Anticoagulant treatment is associated with decreased mortality in severe coronavirus disease 2019 patients with coagulopathy. *J Thromb Haemost* 2020; 18:1094-9.
15. Zhu J, Ji P, Pang J, et al. Clinical characteristics of 3,062 COVID-19 patients: a meta-analysis. *J Med Virol* 2020 April 15 (Epub ahead of print).
16. Porfidi A, Pola R. Venous thromboembolism in COVID-19 patients. *J Thromb Haemost* 2020 April 15 (Epub ahead of print).
17. Scholten EL, Beitler JR, Prisk GK, Malhotra A. Treatment of ARDS with prone positioning. *Chest* 2017;151:215-24.
18. Gu J, Gong E, Zhang B, et al. Multiple organ infection and the pathogenesis of SARS. *J Exp Med* 2005;202:415-24.
19. O'Donnell J, Sharif K, Emery P, Bridgewood C, McGonagle D. Why the immune mechanisms of pulmonary intravascular coagulopathy in COVID-19 pneumonia are distinct from macrophage activation syndrome with intravascular coagulation. April 2020 (https://www.researchgate.net/publication/340621484_Why_the_Immune_Mechanisms_of_Pulmonary_Intravascular_Coagulopathy_in_COVID-19_Pneumonia_are_Distinct_from_Macrophage_Activation_Syndrome_with_Disseminated_Intravascular_Coagulation). preprint.
20. Mentzer SJ, Konerding MA. Intussusceptive angiogenesis: expansion and remodeling of microvascular networks. *Angiogenesis* 2014;17:499-509.
21. Ackermann M, Stark H, Neubert L, et al. Morphomolecular motifs of pulmonary neoangiogenesis in interstitial lung diseases. *Eur Respir J* 2020;55(3):1900933.
22. Buja LM, Wolf D, Zhao B, et al. Emerging spectrum of cardiopulmonary pathology of the coronavirus disease 2019 (COVID-19): report of three autopsies from Houston, Texas and review of autopsy findings from other United States cities. May 7, 2020 (<https://www.science.direct.com/science/article/pii/S1054880720300375>). preprint.
23. Hoffmann M, Kleine-Weber H, Krueger N, Mueller MA, Drosten C, Poehlmann S. The novel coronavirus 2019 (2019-nCoV) uses the SARS-coronavirus receptor ACE2 and the cellular protease TMPRSS2 for entry into target cells. January 31, 2020 (<https://www.biorxiv.org/content/10.1101/2020.01.31.929042v1>). preprint.
24. Yan R, Zhang Y, Li Y, Xia L, Guo Y, Zhou Q. Structural basis for the recognition of SARS-CoV-2 by full-length human ACE2. *Science* 2020;367:1444-8.
25. Varga Z, Flammer AJ, Steiger P, et al. Endothelial cell infection and endothelitis in COVID-19. *Lancet* 2020;395:1417-8.

Copyright © 2020 Massachusetts Medical Society.